MODELING AND IDENTIFICATION OF A HIGH RESOLUTION SERVO, FOR MOBILE ROBOTICS

Ahmed Sachit HASHIM[1], Bogdan GRĂMESCU[2], Adrian Laurenţiu CARTAL[3], Constantin NIȚU[4]

The paper presents the modeling of a servo actuator and the way of conducting some experiments for determining its main physical parameters, when the datasheet does not specify them. The servo actuator is a closed loop positioning system with DC motor and PID control and its model is developed in 20-sim, by help of Bond Graph and Signal libraries. A modified Karnopp friction model is adopted for the friction losses in the gear speed reducer and the simulation for an obstacle avoidance of a mobile robot is presented.

Keywords: servo actuator, Bond Graph modeling, parameter identification.

1. Introduction

Mobile robotics is, probably, the most interesting area of robotic research, approached both by industry and academic environment [1]. There are achievements extending from hobby to space explorers (e.g. Mars exploration rover), passing through many educational demonstrators [2], [3]. For the latter, as well as for hobby developments, there are components, which can satisfy the performance within a good price. As servo actuators, Dynamixel series and XYZrobot A1-16 are relatively new smart actuators from this class. Because both producers do not reveal some internal parameters necessary for modeling their servos, and Dynamixel AX-12A was investigated in [4], the goal of this paper is to characterize the other servo actuator, XYZrobot A1-16.

2. XYZrobot A1-16 servo actuator

A1-16 is a modular rotation actuator, which can provide accurate programmable positions, if the external load is kept within some limits. It consists of a DC motor, a gear train, a feedback position sensor and an embedded control board, for completing the automatic closed loop. It looks identical to the servo

[1] PhD Student, Doctoral School of Mechanical Engineering and Mechatronics, University POLITEHNICA of Bucharest, Romania, e-mail: ahmedhashim774@yahoo.com
[2]Assoc.Prof., [3]Assist.Prof., [4]Prof., Dept.of Mechatronics and Precision Mechanics, University POLITEHNICA of Bucharest, Romania, e-mail:{bogdan.gramescu, constantin.nitu}@upb.ro

Dynamixel AX-12+/A, but it claims to provide higher torques. Both A1-16 and AX-12A servos communicate with the system main controller via a serial bus, which allows a daisy chain connection. Although very useful for control programing, because the user needs only to set the target position and speed, serial communication makes difficult the access for a complete identification of the system physical parameters, especially the ones of the DC motor. The only specified physical parameters of the servo A1-16 are presented in the table 1 [5].

Table 1

Datasheet specifications for XYZrobot A1-16 servo

Specification	Parameters values
Operation voltage	8 ~ 12 V (default)
Maximum speed (no load)	70 ± 10 rpm
Stall torque	25.0 kgf.cm max (at 12 V)
Resolution	0.323°
Reduction Ratio	254
Operating Current	500 mA
Standby Current	300mA (max.)
Operating Temperature	0…40°C
Rotary position feedback	360° continuous rotation and maximum 330° effective position control range

As there is no information, which could clarify some parameters of the motor's equations, they should be determined by experiments and indirect measurements. The resolution value, listed in the datasheet [5] of A1-16 servo, is 0.323°, for a positioning range of 330°. The operating alternative is to make endless turns like any other geared DC motor. If, in the first case, the number of positions is considered to be 1024, the listed resolution is confirmed.

A checkout of the gear ratio was achieved, in spite of the necessary servo dismantling, because partial gear ratios are also needed for calculation of the equivalent inertia. The result of the gear teeth counting is the total gear ratio:

$$\frac{39}{10}\cdot\frac{33}{18}\cdot\frac{30}{9}\cdot\frac{29}{9}\cdot\frac{33}{10}=253.428\approx 254$$

As the A1-16 has a gear reduction of 254:1, it is expected that any kind of torque to be significantly amplified at the output shaft, including the friction torque, which provokes loss of the servo output power.

3. Measurement of the internal friction of the servo

There are several models of the friction, both static and dynamic, some of them already implemented as specific blocks in modeling environments. All the classical models of slipping friction include the most popular theory, belonging to

Coulomb. As shown in fig.1,a, Coulomb theory considers the same absolute value of the friction force/torque, the only change with the relative velocity being the action direction (sign for calculation). The real phenomenon makes a difference between a friction force at zero velocity, when the stiction phenomenon prevents the stationary surfaces putting in motion and a kinetic friction force, at the same zero velocity, but with the value of the Coulombian one, after the actuating force has overcome the stiction (fig.1,c).

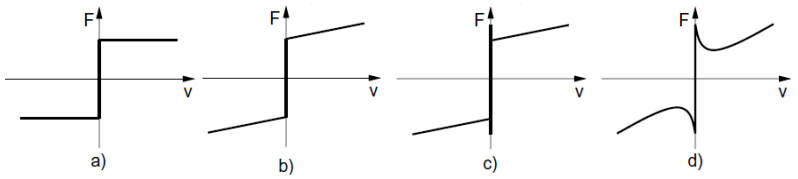

Fig.1. Classical models of friction: a) Coulomb; b) Coulomb and viscous friction (Stribeck); c) Stiction, Coulomb and viscous friction; d) continuous function for model c).

These data are not provided by any producer and they have to be measured and plotted, in the rotation domain, as friction torque against angular velocity. For the stiction friction measurement, the A1-16 servo is fixed into a bench vise, with a lever attached to its rotating hub. The lever is balanced and has a bucket at one end, meant to add small weights until the motion starts (fig.2). The servo is not powered and two metal rings and four screws are added in the bucket, with the total weight of 63 g, in order to put the servo in motion. The balance lever measures l =176 mm, so the static friction torque is: $T_s = mgl = 0.109\ N \cdot m$

Fig.2. Set up for measuring static friction

As the servo's gear train is lubricated by grease, and for identifying a friction model like the one in fig.1,c, the determination of the friction torque values at different velocities is required. For this purpose, another set up is made, consisting of the same servo which is fixed into a bench vise and a grooved wheel, attached to its rotating hub. A wire is wounded in the wheel's groove, with one end fixed on the wheel and the other to a thaler, where calibrated weights can be added (fig.3).

The principle of the indirect measurement of the viscous friction torque is the following: the servo, not power supplied, is put into motion with the wheel and wire, by different calibrated weights, attached to the thaler. This way, the servo is driven at different accelerations over a known distance and the body in

a) b)

Fig.3. a) Experimental set up for measuring the viscous friction torque; b) Detail of the sensors for detecting the moving body

motion is detected when it pass nearby the IR sensors (fig.3,b). The time delay between the signals emitted by the sensors is measured and displayed (fig.3,a). This measurement information is processed for deriving the viscous friction torque, by help of the following equations:

$$T_v = mgr - \left(J_{eq} + mr^2\right) \cdot \varepsilon \tag{1}$$

$$\frac{d}{r} = \varepsilon \frac{t^2}{2} \tag{2}$$

$$\omega_{med} = \frac{\varepsilon \cdot t}{2} \tag{3}$$

where: m – mass attached to the thaler; g – gravity acceleration; r – grooved wheel radius; J_{eq} – equivalent inertia of the moving parts of the A1-16 servo, including the grooved wheel; ε – system angular acceleration; d – distance between IR sensors; t – movement duration of the falling mass, along the distance, d; ω_{med} – average angular velocity on the distance, d; T_v – viscous friction torque, including the kinetic Coulomb component.

Equation (1) describes the dynamics of the system and it needs to be known the time dependence of the acceleration. Supposing a slow variation with velocity of the viscous friction torque, the acceleration can be considered constant (2) and an average velocity can be calculated with (3), in order to put it into accordance with the calculated friction torque. The measurements and calculations results are presented in the fig.4. For this experiment, there were used calibrated masses of 100g and 50g, placed on a thaler with 131g own mass. So, the first driving mass is 481g. The following other data are: $d=0.45$ m; $r = 0.023$ m; $g=9.81$ m/s^2; $J_{eq} = 5.7 \times 10^{-5}$ kg.m^2.

The viscous torque values versus angular velocity are plotted in fig.4, where it is also represented the linear regression line, calculated in Excel. This is the straight line of the friction model in fig.1,c, with the equation:

$$T_v = 0.0082 \cdot \omega + 0.0891 \quad (4)$$

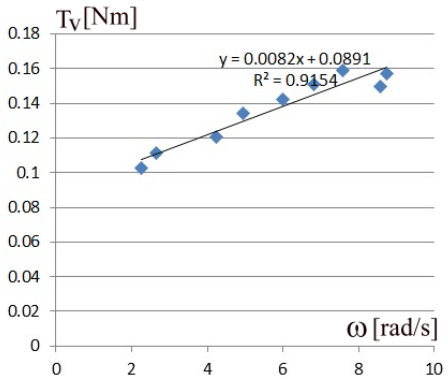

Fig.4.Viscous torque vs. angular velocity

Although no measurement point was discarded, it has a good correlation coefficient $R^2 = 0.9154$. From this equation, an approximation of the value of the Coulomb friction is the free term of (4), namely $T_C = 0.0891$ *N.m.* With these data, the modified Karnopp friction model of the servo actuator can be built (fig.5). This is adequate to the numerical computation, when a zero velocity is hard to be found. Because the stiction phenomenon is important at slow motion, professor Dean Karnopp has introduced a small interval $[-\delta, +\delta]$ of the angular velocity, for which the friction torque is the minimum between $|T_S|$ and $|T_a|$, where T_S is the value of the stiction torque, experimentally determined (T_S=*0.109 N.m*) and T_a is the actuator torque. The actual model differs from Karnopp original one, by the linear variation with the angular velocity, instead of parallel lines to abscissa. In the case of the investigated servo, the friction model is:

$$T_{slip} = \begin{cases} 0.0891+0.0082.\omega & \text{if } \omega \geq \delta \\ -0.0891 - 0.0082.\omega & \text{if } \omega \leq -\delta \end{cases} \quad (5)$$

$$T_{stick} = \begin{cases} \min(T_a, T_S) & \text{if } -\delta < \omega < \delta \text{ and } T_a \geq 0 \\ \max(T_a, -T_S) & \text{if } -\delta < \omega < \delta \text{ and } T_a \leq 0 \end{cases} \quad (6)$$

4. Mechanical characteristic of the A1-16 servo

The mechanical characteristic of a servo with DC motor is the family of the torque versus angular velocity diagrams, at different voltages (fig.6). Because a servo includes an assembly motor-gearbox, the torque will be multiplied by the gearbox ratio, while the angular velocity will be diminished with the same ratio. This means that the torque constant, k is the product between the motor torque constant and the gear ratio. As the diagram torque vs. angular velocity makes use

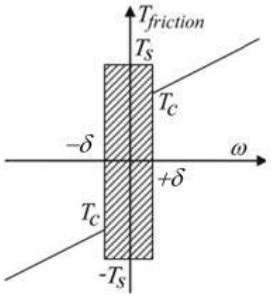

Fig.5. Karnopp modified model of friction

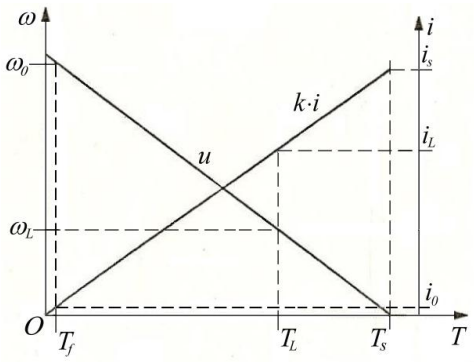

Fig.6. General characteristic of a DC motor

of the output velocity of the gear box, the back emf constant is also the same.

The new test of the XYZ servo is based on these considerations, and measures the angular velocity of the servo, loaded with different masses, while it is power supplied at different voltages. The current consumption of the servo is also measured. The set up for these trials is presented in fig.7. It consists of the servo fixed in a bench vise and with the grooved wheel attached to its rotating hub. The wire wounded around the wheel has an end attached to the wheel and the other linked to a thaler, for calibrated masses.

The servo is supplied at 8, 10 and 12 V and the current consumption and angular velocity are recorded. The same test is performed, but the servo is loaded with 1.121 kg and 2.036 kg respectively, while the current and angular velocities are recorded during raising the weights. The results of the tests are presented in the table 2.

The goal of this test is to find out the total resistant torque, which is denoted by T_L in fig. 6, meaning that both the useful load (raised by the wire) and the internal friction have a contribution to the absorbed current value.

As it is shown in fig.6, an i_L current corresponds to the torque T_L and their ratio is *k*, the torque/back emf coefficient. For calculation of the total load torque values, equation (5) was used to determine the internal viscous friction torque and the torque generated by the added masses was calculated with:

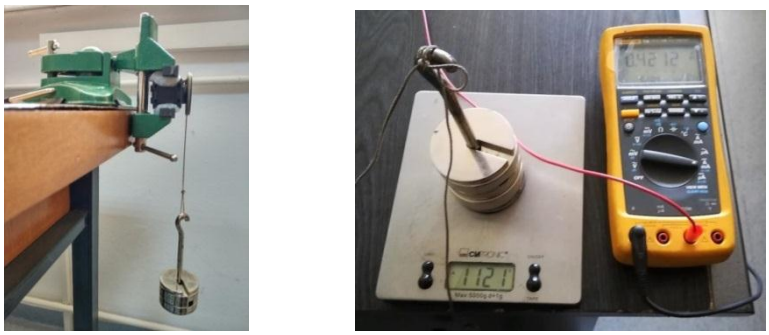

Fig.7. Set up for determination of the servo characteristic

Table 2

Absorbed current for different load torques

Load [kg]	**Voltage [V]**	**Current [A]**	**Number of turns [rpm]**	**Angular speed [rad/s]**	**Gravity torque (T_G) [Nm]**	**Friction torque (T_v) [Nm]**	**Load torque (T_L) [Nm]**
0	8.1	0.192	48.59	5,19	0	0.13166	0.13166
0	10.1	0.222	58.77	6.15	0	0.13953	0.13953
0	11.8	0.227	69.18	7.24	0	0.14847	0.14847
1.121	8	0.427	40.41	4.23	0.26943	0.12379	0.39322
1.121	10	0.434	42.86	4.49	0.26943	0.12592	0.39535
1.121	12	0.495	60.61	6.35	0.26943	0.14117	0.41060
2.036	8	-	-	-	-	-	-
2.036	10	0.656	42.86	4.49	0.48934	0.12592	0.61526
2.036	11.8	0.689	48.37	5.07	0.48934	0.13067	0.62001

$$T_G = m \cdot g \cdot r \tag{7}$$

where: m – mass of the additional weights; g – gravity acceleration; r – radius of the grooved wheel.

In fig.8, the values of the total load torque and the corresponding current are plotted and the regression line is determined with a very good confidence (R

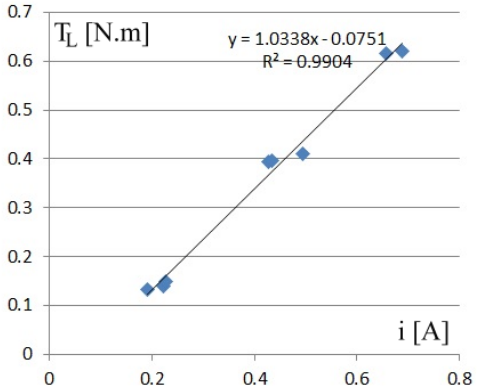

Fig.8. Torque vs. current diagram

square: 0.9904). It results from the equation that *k* coefficient has the value of the line slope, *k = 1.034 N.m/A*. Moreover, the line crosses the abscissa axis very close to zero, which is almost like the theoretical representation in fig. 6.

The last important parameter which is necessary for servo modeling is the electrical resistance of the DC motor armature. It cannot be measured directly without servo dismantling, so the stall torque of the servo, given by its datasheet, is used: $T_s = 25kgf \cdot cm = 2.45\ N \cdot m$, at 12 V. Knowing that,

$$T_S = k \cdot i_S = k \cdot \frac{u}{R}\ , \tag{8}$$

the electric resistance of the motor armature is: $R = \frac{k \cdot u}{T_S} = \frac{1.034 \cdot 12}{2.45} = 5.06\ \Omega$

The stall current is: $i_S = \frac{T_S}{k} = \frac{2.45}{1.034} = 2.37\ A$. The obtained value is credible, because the producer has limited the working current of the servo at 2A.

5. Reminder of Bond Graphs modeling

Bond Graphs are a graphical modeling language, created by Prof. H.M. Paynter from Massachusetts Institute of Technology, in 1959, which graphically describe the dynamic behavior of the physical systems. The models are built with a unique system of notation, used for each physical domain, based on the energy transfer between the components of the physical system. This is a powerful modeling mean for engineering systems, especially for the interdisciplinary ones. Many other researcher have contributed to the development of the method and software environments, adequate for graphical modeling, like 20-sim, Dymola, Symbols 2000. The main idea is to represent the physical systems with their properties to generate, store, dissipate or transform power, with components having lumped parameters and power variables, linked by half arrows, called bonds, which indicate the positive power flow direction. Each bond is associated with two power variables, which are generically called *effort* and *flow*. Depending on the physical domain, they can be:

- in the electrical domain – voltage (effort) and current (flow);
- in the mechanical domain (translation) – *force (effort) and velocity (flow);*
- in the mechanical domain (rotation) – *torque (effort) and angular velocity (flow).*

The point of a physical system, where the power is transferred between two components is called *port*. In fig.9, there are shown four one-port components of the Bond Graph formalism: S_e - source of effort (actuator force); *C* – compliance (spring compliance); *R* – resistance (damping coefficient); *I* – inertia (oscillating mass). Another component is a multiport element - the junction *-1*, which is characterized by a *common flow*.

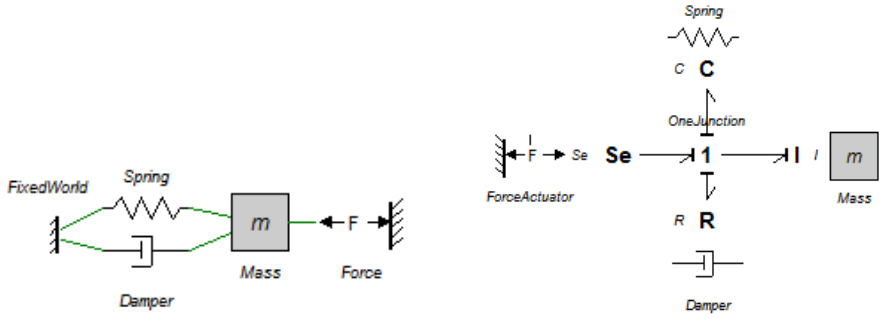

a) b)

Fig.9. Mass-spring-damper oscillator: a) physical model; b) Bond graph model

In these circumstances, the power conservation law ($\sum_{k=1}^{n} e_k \cdot f_k = 0$) becomes

$$\sum_{k=1}^{n} e_k = 0 \tag{9}$$

The equation (9) and, implicitly, the junction *-1* replace d'Alembert equation in the mechanical domain and second Kirchhoff law, in the electrical domain. A complementary multiport, junction – *0*, is characterized by a *common effort*, which leads to the equation:

$$\sum_{k=1}^{n} f_k = 0 \tag{10}$$

The Bond Graph formalism has 9 basic elements, which are:

- S_e, S_f – sources of effort or flow, single-port elements; for example, a battery is a source of voltage, gravity is a source of force, and a pump is a source of fluid flow; in the real applications, there are used modulated sources, MS_e and MS_f, which are two-port elements, with signal input and power output; this way, the output of MS_e and MS_f can vary according to the signal mathematical law;
- *I, C* – single-port energy storage elements, with the constitutive equations:

$$f = \frac{1}{I}\int e \cdot dt \tag{11}$$

$$e = \frac{1}{C}\int f \cdot dt \tag{12}$$

- *R* – single-port energy dissipative element, with the constitutive equations:

$$e = R \cdot f \quad \text{or} \quad f = \frac{e}{R} \tag{13}$$

- *TF* – two - ports element (transformer), which transforms the values of the input variables, into the same type of output variables, with a constant and inverse ratio:

$$e_o = n \cdot e_i \tag{14}$$

$$f_o = \frac{1}{n} \cdot f_i \tag{15}$$

In the mechanical domain, gears, timing belts and chain transmissions are transformers; sometimes, as in the case of planar mechanisms, the transformer

ratio can vary with a parameter (regularly, the position), when the bond graph element is a modulated transformer (MTF);
- *GY* - two - ports element (gyrator), which transforms the values of the input variables, into the other type of output variables, with a constant and inverse ratio:

$$e_o = n \cdot f_i \tag{16}$$

$$f_o = \frac{1}{n} \cdot e_i \tag{17}$$

An example of gyrator is the ideal DC motor ($T=k.i$ *and* $u=k.\omega$)

- *1* and – *0* junctions are multiport elements, which connect the other elements for power transfer.

The constitutive equations (11), and (12) can be also written into the derivative form, but this is not recommended when numerical methods are used. In order to indicate how is interpreted the constitutive equation of one element, a causal stroke is added to the bond half arrow. If the *I* component should have nearby the causal stroke (at the half arrow), for an integrative constitutive equation, the *C* component should have the causal stroke on the opposite side of its bond. Additional causality rules are to be respected by sources of efforts and flows. So, an effort source has always the causality stroke, opposite to the effort source. For the flow source, the situation is vice-versa and the causal stroke is at the end of the bond, near the flow source.

6. Modeling of the actuator XYZrobot A1-16

The model of the servo actuator XYZ A1-16 is a simplified approach, where the actual PWM control of the DC motor is considered a current control, and the digital PID controller is replaced by a continuous one (fig.10). The winding inductance was not measured/determined, because it has no significance, when the motor is current controlled. The model exploits the 20-sim facility of combining the Signal library with the Bond Graph one, which is based on power variables [6].

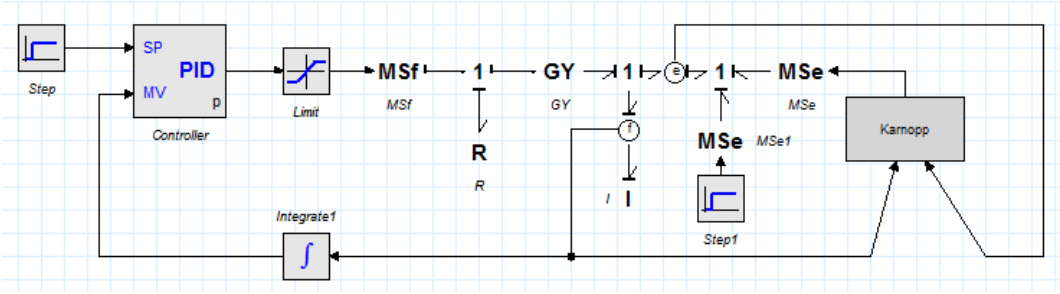

Fig.10. Simplified model of the loaded servo A1-16 in 20-sim

The transition between the signal domain and the power domain is

achieved by special components of the Bond Graph domain: ***MSf*** – modulated flow source - a flow source, controlled by a signal value; ***MSe*** - modulated effort source - a effort source, controlled by a signal value; ***Flow sensor*** and ***Effort sensor*** – components extracting only one of the power variables of a bond, in order to be used as signal;

The other components of the simulation scheme from figure 10 have the following roles: ***Step*** – reference value of the angular position; ***Step 1*** – load torque provided by the actuated mechanism; ***Plus-minus (comparator)*** – creates the error signal between the reference and the feedback, generated by the flow sensor; ***Limit*** block – limits the motor current slightly below its stall value; ***Karnopp*** block is an equation submodel specially built in 20sim by the authors, in order to implement the stiction and viscous internal friction of the servo A1-16, as expressed in (5), (6), after experiments; ***Integrate operator*** on the feedback loop – transforms the angular velocity, measured by the flow sensor into angular position. The graphic model has also the components, $R=5.06\ \Omega$ - rotor winding resistance and GY, whose ratio is $k= k_t = k_\omega =1.034\ N.m/A$. I is the equivalent inertia of the servo and the actuated mechanism; for the not loaded actuator, $I= J_{eq} = 5.7x\ 10^{-5} kg.m^2$- the equivalent inertia of the motor rotor and gears, at the output shaft.

The model from fig.10 use a PID_p controller from the Signal library of 20-sim, which means a parallel form of the PID controller with the following transfer function:

$$C(s) = \frac{u}{\varepsilon} = K\left(1 + \frac{1}{T_i s} + \frac{T_d s}{1+\frac{T_d}{N}s}\right) \tag{18}$$

where: u – output of the controller (command signal); $\varepsilon = SP\text{-}MV$ – error signal; K – proportional controller gain; T_i - integral time constant ($T_i > 0$); T_d - derivative time constant ($T_d > 0$); N – derivative gain limitation.

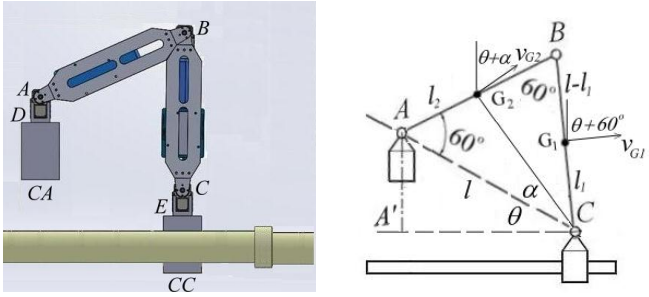

Fig.11. Active joint C, powered by servo actuator A1-16, raising the robotic arms AB and BC

If the analyzed servo actuator is placed in joint C of the robot from fig.11, it should raise the arm BC, with 30° (θ in fig.11) while the triangle ABC is kept equilateral, in order to overpass a flange/bracket encountered on a pipe [7]. This is

the case in which one actuator of the robotic structure is maximum loaded, both inertial and by torques caused by gravity forces, when $\theta = 0°$. The equivalent moment of inertia is $J_{eqmax} = 2.325 \cdot 10^{-2} kg \cdot m^2$ and the equivalent gravity torque is $T_{reqmax} = 2.1 \ N \cdot m$. The simulation result, run with these values and PID parameters, *K=10*, *N=100*, T_i*=1.6s* and T_d*=0.5s* is presented in fig.12.

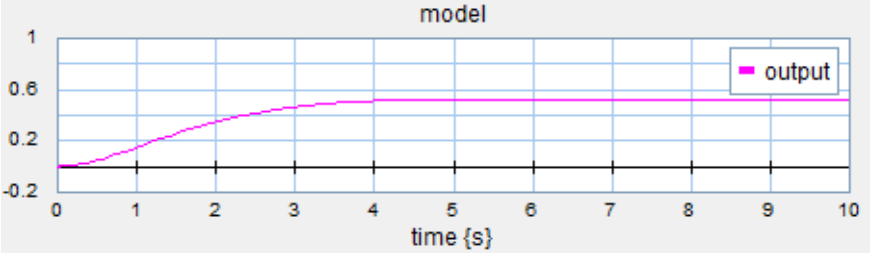

Fig.12. Position response of the robotic chain [rad], for a 30° step reference (initial position 0°)

It shows that the actuator is able to raise the robotic chain to the reference position in maximum 5 seconds, with a resistant torque close to its stall one.

7. Conclusions

The paper addresses to students and other developers of mobile robots, which use servos as actuators in their projects. It helps them with new and minimum invasive methods to determine the internal friction torque and the torque coefficient of the DC motor inside the servo and proposes a modified Karnopp model of friction.

The actuator model is also unusual, because it is developed in Bond Graph language, within the 20-sim environment and its simplicity should convince that this tool is valuable for mechatronic systems.

R E F E R E N C E S

[1]. *R. Siegwart, I.R. Nourbakhsh* – Introduction to Autonomous Mobile Robotics MIT Press Cambridge, Massachusets, ISBN 0-262-19502-X, 2004

[2]. *B. Crnokić, M. Grubišić and T. Volarić* - Different applications of mobile robots in education, in International Journal on Integrating Technology in Education (IJITE) Vol.6, No.3, September 2017

[3]. *P. Wiesen, H. Engemann, N. Limpert, S. Kallweit* - Learning by Doing - Mobile Robotics in the FH Aachen ROS Summer School, in TRROS 2018 – European Robotics Forum 2018 Workshop "Teaching Robotics with ROS", pp.47-58

[4]. *A. Mensink* - Characterization and modeling of a Dynamixel servo – Individuel Research Assignment – University of Twente, Enschede, 2008, The Netherlands

[5]. *** https://www.pololu.com/product/3400

[6]. *** 20-sim 4.0 – Reference Manual, Controllab Products B.V., 2008.

[7]. *A.S.Hashim* – Robot for External Inspection and Monitoring of the Oil and Gas Pipes, PhD Thesis, University "POLITEHNICA" of Bucharest, 2019